

## Multiple Avalanches across the Metal-Insulator Transition of Vanadium Oxide Nanoscaled Junctions

Amos Sharoni,<sup>1,\*</sup> Juan Gabriel Ramírez,<sup>1,2</sup> and Ivan K. Schuller<sup>1,†</sup>

<sup>1</sup>*Physics Department, University of California-San Diego, La Jolla California 92093-0319, USA*

<sup>2</sup>*Thin Film Group, Universidad del Valle A.A.25360, Cali, Colombia*

(Received 5 March 2008; published 11 July 2008)

The metal-insulator transition of nanoscaled VO<sub>2</sub> devices is drastically different from the smooth transport curves generally reported. The temperature driven transition occurs through a series of resistance jumps ranging over 2 decades in magnitude, indicating that the transition is caused by avalanches. We find a power law distribution of the jump sizes, demonstrating an inherent property of the VO<sub>2</sub> films. We report a surprising relation between jump magnitude and device size. A percolation model captures the general transport behavior, but cannot account for the statistical behavior.

DOI: [10.1103/PhysRevLett.101.026404](https://doi.org/10.1103/PhysRevLett.101.026404)

PACS numbers: 71.30.+h, 64.60.an, 64.60.Ht, 72.80.Ga

There are many systems in nature that have a transition from one state to another which is driven by an external force, where the transition is not continuous, but rather through a series of avalanches. These systems are diverse as is the driving force and the measurement technique used to observe them. Examples include Barkhausen noise in ferromagnets [1,2], acoustic emission in martensitic transitions [3,4], the magnetocaloric effect in giant magnetocaloric alloys [5], sharp magnetization steps or sharp resistance steps in manganites [6,7], vortex avalanches in superconductors [8], and capillary condensation of He in nanoporous material [9]. In general an external parameter modifies the free energy of the two phases, which provides the driving force for the system. The nature of the avalanches provides much information about the system at hand. One can learn about the types of interaction, the role of fluctuations, the existence of self organized criticality, and the universal features of the transitions which transcend the specific physical system [4,10–12].

Several of these systems are characterized by phase separation during the transition. This implies that the transition occurs through a series of avalanches transforming portions of the system from one phase to the other [13–15]. One such system, which has received much attention, is vanadium oxide (VO<sub>2</sub>). VO<sub>2</sub> undergoes a first order metal-insulator transition (MIT) of over 4 orders of magnitude at ~340 K. The transition is from a high temperature metallic rutile phase to a low temperature insulating monoclinic phase, and can be driven by temperature, light irradiation or pressure [16]. In this Letter we report the first observation of multiple avalanches across the temperature driven MIT in VO<sub>2</sub>. Avalanches may be expected in this system for multiple reasons; it has a first order phase transition; there is a state of phase separation between metallic and insulating regions along the transition [17,18]; and ultrafast measurements reveal a phase transition in separated domains of the system with a transition time on the order of a few picoseconds [19,20].

Generally, in order to identify an avalanche, the resolution of measurement has to be greater than the magnitude change of the relevant parameter, and the measurement sampling rate higher than the avalanche frequency [2,3,21]. For resistance measurements in VO<sub>2</sub> this implies that the size of the device has to be comparable to the magnitude of the domains involved in a single event, and that the rate of change of the driving force slow enough to resolve the avalanches.

By measuring transport properties of VO<sub>2</sub> devices, with electrode spacing as small as 200 nm and temperature sweeping rates lower than 3 K/min, we were able to detect that the MIT evolves through a series of discreet jumps ranging over two decades of resistance indicating the transition is through a series of avalanches. We find a scaling law which shows that the magnitudes of the largest jumps are inversely proportional to the device length. Interestingly the jump size distribution follows a power law which is generally robust for various important parameters, including different depositions, device size, and temperature sweep rates. The general shape of the transport measurement can be understood in the framework of a noninteracting site percolation model. But it cannot explain the statistical nature of the jump sizes, implying that the power law distribution is an expression of an intrinsic property of the VO<sub>2</sub> films.

Vanadium oxide thin films were prepared by reactive rf magnetron sputtering of a vanadium target (1.5" diameter, >99.8%, ACI Alloys, Inc.) on an *r*-cut sapphire substrate. The samples were prepared in a high vacuum deposition system with a base pressure of  $5 \times 10^{-8}$  Torr. A mixture of ultrahigh purity (UHP) argon and UHP oxygen gasses were used for sputtering. The total pressure during deposition was  $3 \times 10^{-3}$  torr, and the oxygen partial pressure was optimized to  $1.5 \times 10^{-4}$  torr (5% of the total pressure). The substrate temperature during deposition was 500 °C while the rf magnetron power was kept at 300 W. These conditions yielded a deposition rate of 0.37 Å/s, and

a total thickness of 90 nm was deposited for all the samples reported here. The samples were cooled at a rate of  $13^\circ\text{C}/\text{min}$  in the same  $\text{Ar}/\text{O}_2$  flow of the deposition. Films were characterized and verified to be single phase  $\text{VO}_2$  by x-ray diffraction (Rigaku RU-200B diffractometer) using  $\text{Cu } K\alpha$  radiation and energy-dispersive x-ray spectroscopy (Phillips XL30 ESEM). Macroscopic measurements of resistance vs temperature ( $R - T$ ) curves reveal an MIT starting at  $\sim 340$  K with a change of almost 4 orders of magnitude in the resistance, indicative of high purity thin films [22].

The  $\text{VO}_2$  nanostructures were fabricated by standard  $e$ -beam lithography and lift-off techniques. On top of the  $\text{VO}_2$  film metallic electrodes were deposited by sputtering 50 nm vanadium, which acts as an adhesion layer, and 100 nm of gold to assure that the electrode resistance is lower than that of the metallic  $\text{VO}_2$ . Device length was varied between 200 nm to  $4\ \mu\text{m}$  and width from 2 to  $15\ \mu\text{m}$ . A typical sample with 8 devices is depicted in Fig. 1(a) (see caption for details). Using standard photolithography, the rest of the  $\text{VO}_2$  was etched in argon plasma, leaving only a square of  $\text{VO}_2$  (clearly seen in Fig. 1(a)). In the final step the electrodes were photolithographically connected to macroscopic pads. The  $R - T$  characteristics were acquired in a home made test-bed by standard 2 probe or quasi 4 probe measurements (with no significant difference between the two) using a constant current source at a measurement rate of 10 Hz. Temperature was controlled by a Lakeshore 332 temperature controller, with sweep rates varying between  $0.1\ \text{K}/\text{min}$  and  $3\ \text{K}/\text{min}$ . Each measurement was cycled multiple times (10–100) in order to obtain sufficient data for statistical analysis of the jumps.

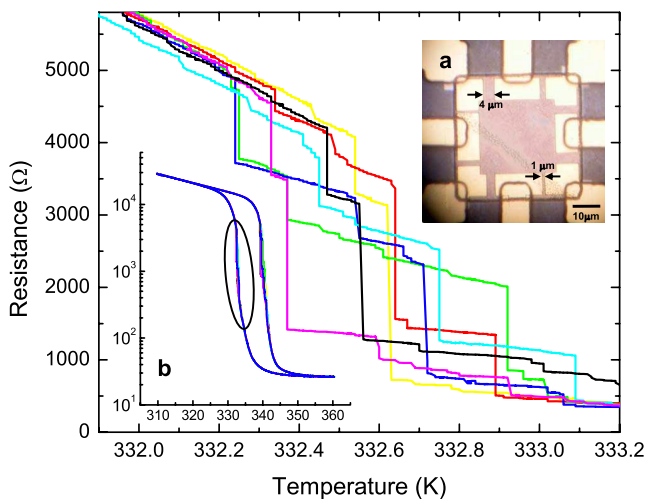


FIG. 1 (color online). Main panel—8 consecutive  $R - T$  cycles ( $R$  in linear scale) of a  $1 \times 6\ \mu\text{m}^2$   $\text{VO}_2$  device zoomed in on part of the MIT, as marked in the full measurement shown in (b) (log scale of  $R$ ). (a)—Image of 8 devices on one sample showing  $\text{VO}_2$  square of side  $50\ \mu\text{m}$ , on top of which are V/Au electrodes defining device lengths of 1, 2, 3, and  $4\ \mu\text{m}$  (2 devices of each) and width of  $8\ \mu\text{m}$  for all the devices. Devices with length of 1 and  $4\ \mu\text{m}$  are marked.

Figure 1 (main panel) shows 8 consecutive cycles of a typical  $R - T$  measurement across a  $1 \times 6\ \mu\text{m}^2$  device focusing on the numerous resistance jumps (cooling curves). The full range measurement is depicted in Fig. 1(b). The transition temperature is 338 K (for heating) and the total change in resistance is over 3 orders of magnitude occurring along  $\sim 8$  K with a typical hysteresis of 7 K, which is similar to the macroscopic properties of the sample. The jumps range from over 2000  $\Omega$  for the largest jumps to below 10  $\Omega$ , limited only by the measurement noise. We find that the jumps occur between two consecutive measurements even for the slowest temperature sweep rates, where the (nominal) temperature change between adjacent data points is smaller than 0.5 mK. This indicates that the time scale of each jump is much shorter than our measurement capabilities, which is expected due to the fast nature of the  $\text{VO}_2$  transition, of a few picoseconds [19,20]. This implies that the transition between the spatially separated but coexisting metallic and insulating phases in  $\text{VO}_2$  [17,18] is not continuous, but rather occurs through a series of avalanches, where each avalanche is expressed as a resistance jump in the measurement.

The main characteristics of the  $R - T$  measurement are as follow: the first jumps appear close to the onset temperature of the macroscopic transition. There are 1–3 large jumps (ranging up to a few thousands of ohms in some cases), which may account for 50% of the resistance change. The rest of the jumps are smaller, from a few hundred ohms and are limited by the resolution of our measurement. In some samples, jumps as small as 2  $\Omega$  were resolvable. Figure 2 shows the three largest jumps (each one averaged over at least 10 cycles and 2 devices) as a function of the device length. Interestingly, the largest jump decreases with device length and is a linear function

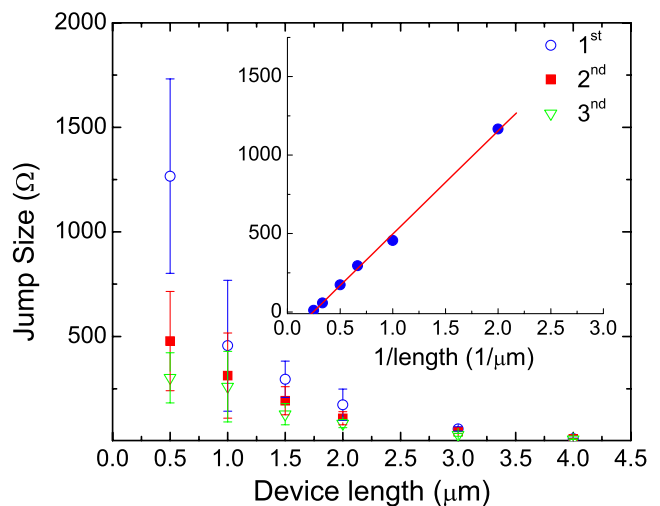


FIG. 2 (color online). Average value of each of the three largest jumps as a function of device length. The inset plots only the average of the largest jump as a function of inverse the device length. Error bars are standard deviations.

of inverse the device length, as demonstrated in the inset of Fig. 2. By extrapolating the linear relation presented in the inset of Fig. 2 to a jump size of zero we find that the  $R - T$  would look smooth for electrode spacing of over 6 microns. This may explain why avalanches were not observed in other experiments performed on devices longer than  $10 \mu\text{m}$ .

The interesting nature of the avalanches is illustrated by the size distribution of the jumps measured along the phase transition. Figure 3 (main panel) shows a histogram of the sizes of the jumps, taken from over 100 cycles, measured for a  $1 \mu\text{m}$  device at a rate of  $1.2 \text{ K/min}$ . The histogram fits well to a power law,  $p(A) \propto A^{-\alpha}$ , where  $p$  is a probability function and  $A$  is the size of the jump. The value of  $\alpha$  was derived using the maximum likelihood method [23] and is found to be  $2.48 \pm 0.05$ . Figure 3(a) depicts exponent values for different device lengths, while  $\alpha$  as a function of the temperature ramp rate is presented in Fig. 3(b). The value of  $\alpha$  has some dependence on device length while it does not change considerably with temperature ramp rate. In addition we find that the power law behavior is identical for heating and cooling. To a first approximation, the value of the exponent is of similar magnitude in all these samples, and is not strongly affected by any of the parameters tested. Thus, this measured exponent is an inherent and characteristic property of the  $\text{VO}_2$  thin films.

We find evidence for an athermal transition; i.e., thermal fluctuations do not play an important role in the MIT. We monitored the resistance at constant temperatures along the

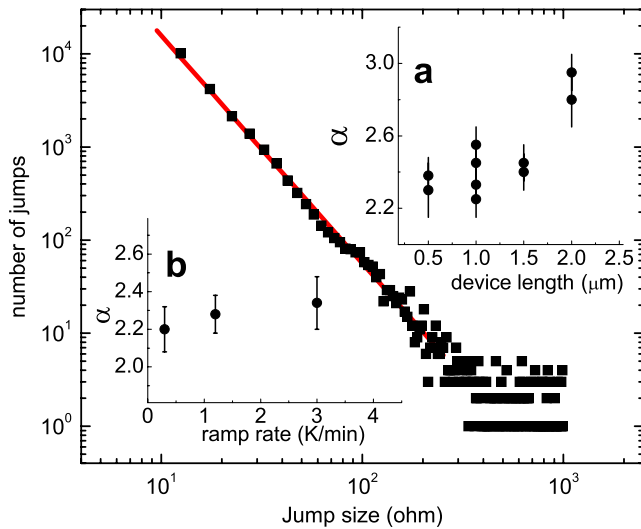


FIG. 3 (color online). Histogram of the jump sizes plotted on a log-log scale, acquired from over 100 cycles measured for a sample  $1 \times 6 \mu\text{m}^2$ . Solid line (red online) is calculated using the maximum likelihood method, indicating a power law dependence. The exponent  $\alpha = 2.48 \pm 0.05$ . a-  $\alpha$  for different channel lengths from different samples. Data for the  $1 \mu\text{m}$  device are provided from 3 different samples deposited under the same nominal conditions (on one sample 2 devices were measured). b-  $\alpha$  as a function of temperature ramp rate.

transition. In most cases, like the one presented in Fig. 4(a), there are no jumps when the temperature is constant. This figure shows that while the temperature is ramped at a rate of  $0.2 \text{ K/min}$  for the first 5 min (top curve and right axis) there are a number of avalanches and large changes to the resistances (bottom line and left axis). But once the temperature is stable, during the next 4 hours of measurement there are no avalanches. There were a few cases where we did observe a single event even though the temperature was stabilized. In addition, as pointed out earlier,  $\alpha$  does not vary much as a function of the temperature ramp rate [11].

The observed few large jumps and many smaller jumps with a wide range can be understood in the framework of a percolation network subject to two constraints. First, the resistivity ratio between the insulating and metallic phases is large but finite (in our case  $\rho_I/\rho_M \sim 1000$ ) and second, the area measured is finite, so the total number of domains which transit through an avalanche is not very large (on the order of  $\rho_I/\rho_M$ ). In order to model the effects of percolation in the experimental system we performed numerical simulations of a site percolation model on a square lattice

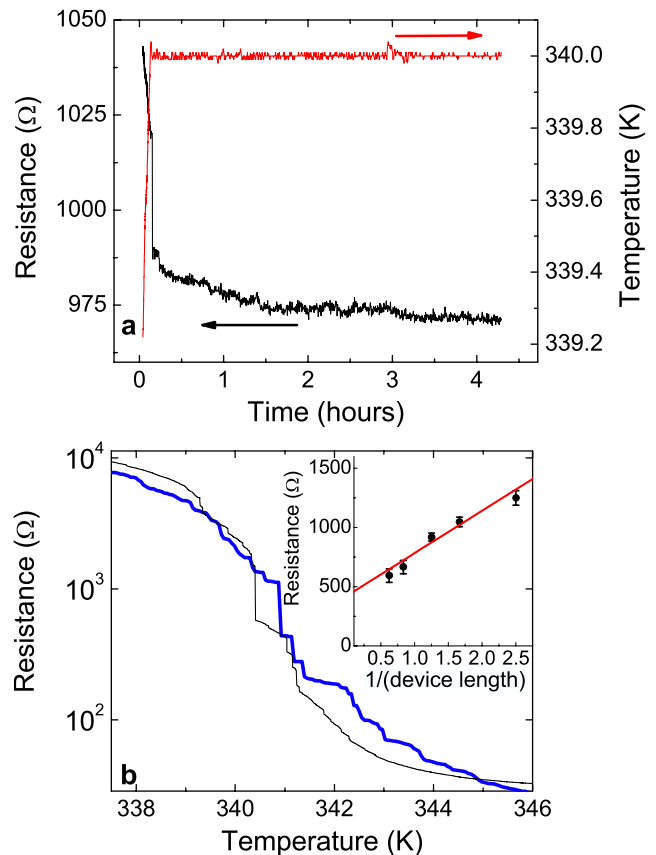


FIG. 4 (color online). a- Resistance (bottom curve, left axis) and temperature (top curve, right axis) as a function of time. No avalanches are observed for constant temperatures. b- Simulation of  $R - T$  (thick line, blue online) along with experimental data (thin line, black) from a  $1 \times 6 \mu\text{m}^2$  device, cooling branch. The simulation is of size  $20 \times 50$  (length  $\times$  width) on a square lattice and  $\rho_I/\rho_M = 1000$ .

with nearest neighbor bonds. This is reasonable, since the macroscopic VO<sub>2</sub> MIT can be modeled by an effective medium approximation [24]. In our simulations each site changes randomly from a finite metallic resistance to a finite insulating one and the resistances of all the sites are identical. Figure 4(b) portrays a simulation with conditions similar to the experimental values. The thick (blue online) line is the simulation, while the thinner one is an experimental  $R - T$ . It is evident that this simple model captures the main features of the experimental data. We can identify with certainty the largest jump in the experiment as the percolation threshold. The magnitude of the percolation jump for different device geometries, averaged over 200 realizations, scales with inverse the device length in a similar fashion to the experiment [shown in the inset of Fig. 4(b)]. But, in the simulation, the average jump size is non zero even for the longer devices.

In the attempt to understand the statistics of the avalanches, it is important to note that the size of a resistance jump is not a direct measure of the VO<sub>2</sub> volume involved in an avalanche event. Rather, this magnitude is superimposed on the percolation nature of the measurement. This can be seen in the simulations [Fig. 4(b)], where a wide distribution of jump sizes is evident even though we assumed that all the sites have identical properties. We investigated the contribution of only the percolation to the power law distribution of the avalanches. In order to do that we calculated values of  $\alpha$  for device geometries similar to the experimental one and in the same fashion as we did for the experimental data. We find that the value of  $\alpha$  varied considerably, between 1.2 and 3.5, for different simulation sizes and for different cutoffs in the most likelihood analysis. For the numerical simulations, the log-log plot of the jump size histograms shows that the number of jumps becomes constant and the slope flattens with decreasing jump size. Thus, only a small part of the data range fits a power law (linear slope) dependence. This means that the distribution function of the numerical data is not a power law, and the experimental data cannot be explained solely by the geometrical nature of percolation. In order to account for the distribution of avalanches one has to take under consideration intrinsic properties of the VO<sub>2</sub> system, interactions, inhomogeneities in the sample, or in the driving force. This work is beyond the scope of the current Letter.

In summary, by choosing a properly nanostructured film we were able to observe discrete transitions in the metal-insulator transition of VO<sub>2</sub> films. These results imply that the metal-insulator transition occurs through a series of

avalanches. The largest of these discontinuous transitions has an inverse dependence with sample size. Importantly, the power law dependence cannot be explained only by the percolation nature of the measurement, meaning that the statistics capture a characteristic property of vanadium oxide thin films, which may be a signature of self organized criticality [25].

We thank Harry Suhl, Fèlix Casanova and María Elena Gómez for fruitful discussion and Yonatan Dubi for his help with the numerical simulations. This work was supported and funded by the U.S. Department of Energy and the AFOSR.

---

\*asharoni@physics.ucsd.edu

†ischuller@ucsd.edu

URL: <http://ischuller.ucsd.edu/>

- [1] P. J. Cote and L. Meisel, Phys. Rev. Lett. **67**, 1334 (1991).
- [2] E. Puppim, Phys. Rev. Lett. **84**, 5415 (2000).
- [3] E. Vives *et al.*, Phys. Rev. Lett. **72**, 1694 (1994).
- [4] L. Carrillo *et al.*, Phys. Rev. Lett. **81**, 1889 (1998).
- [5] F. Casanova *et al.*, Appl. Phys. Lett. **86**, 262504 (2005).
- [6] R. Mahendiran *et al.*, Phys. Rev. Lett. **89**, 286602 (2002).
- [7] S. Hébert *et al.*, Solid State Commun. **122**, 335 (2002).
- [8] E. Altshuler *et al.*, Phys. Rev. B **70**, 140505(R) (2004).
- [9] M. P. Lilly, P. T. Finley, and R. B. Hallock, Phys. Rev. Lett. **71**, 4186 (1993).
- [10] K. S. Ryu, H. Akinaga, and S. C. Shin, Nature Phys. **3**, 547 (2007).
- [11] F. J. Pérez-Reche *et al.*, Phys. Rev. Lett. **93**, 195701 (2004).
- [12] C. Tang and P. Bak, Phys. Rev. Lett. **60**, 2347 (1988).
- [13] K. H. Ahn, T. Lookman, and A. R. Bishop, Nature (London) **428**, 401 (2004).
- [14] M. Fath *et al.*, Science **285**, 1540 (1999).
- [15] M. Matsukawa *et al.*, Phys. Rev. Lett. **98**, 267204 (2007).
- [16] M. Imada, A. Fujimori, and Y. Tokura, Rev. Mod. Phys. **70**, 1039 (1998).
- [17] M. M. Qazilbash *et al.*, Science **318**, 1750 (2007).
- [18] Y. J. Chang *et al.*, Phys. Rev. B **76**, 075118 (2007).
- [19] V. A. Lobastov, J. Weissenrieder, J. Tang, and A. H. Zewail, Nano Lett. **7**, 2552 (2007).
- [20] A. Cavalleri *et al.*, Phys. Rev. Lett. **87**, 237401 (2001).
- [21] H.-Y. Zhai *et al.*, Phys. Rev. Lett. **97**, 167201 (2006).
- [22] D. H. Kim and H. Kwok, Appl. Phys. Lett. **65**, 3188 (1994).
- [23] H. Bauke, Eur. Phys. J. B **58**, 167 (2007).
- [24] J. Rozen, R. Lopez, R. F. Haglund, and L. C. Feldman, Appl. Phys. Lett. **88**, 081902 (2006).
- [25] P. Bak, C. Tang, and K. Wiesenfeld, Phys. Rev. Lett. **59**, 381 (1987).